



Prateek Sharma · Stefan Diebels

A mixture theory for the moisture transport in polyamide

Received: 29 October 2020 / Accepted: 28 April 2021
© The Author(s) 2021

Abstract Polyamide exhibits hygroscopic nature and can absorb up to 10% of moisture relative to its dry weight. The absorbed moisture increases the mobility of the molecular chains and causes a reduction in the glass transition temperature. Thus, depending on the moisture distribution, a polyamide component can show different stiffness and relaxation times. Moreover, the moisture distribution also depends on the mechanical loading of the material as the volumetric deformation results in a change of the available free volume for the moisture. Thus, a strongly coupled model is required to describe the material behaviour. In this work, a thermodynamically consistent coupled model within the framework of mixture theory is developed. The mechanical deformation of polyamide 6 (PA6) is based on a linear viscoelastic material model, and the moisture transport is based on a nonlinear diffusion model. The stiffness and the relaxation time of the viscoelastic model change with the moisture concentration. Furthermore, the moisture transport is affected by the pressure gradient generated by the mechanical loading of the material. This strongly coupled model has been implemented using the finite element method, and simulation results are presented for a three-point bending experiment.

Keywords Two-phase model · Superimposed continua · Viscoelasticity · Moisture transport · Thermodynamic consistency

1 Introduction

Technical polymers such as polyamide (PA6) form a major portion of the polymer applications. Due to its mechanical durability and chemical resistivity, PA6 is used under various environmental conditions, where the temperature and humidity can vary with time. As it is hygroscopic in nature, it can absorb from 9.5 to 10% of moisture by weight [1, 2, 10]. The diffusion of water in the polyamide depends on various parameters such as temperature, loading conditions and time. The presence of moisture can increase the PA6 chain mobility altering its mechanical behaviour [6, 9, 25]. One of the effects of the moisture absorption is that the effective stiffness of the material decreases which has been seen in experimental results [6, 9, 17]. Further, the moisture uptake behaviour is also effected by the loading as the free volume between the polymer chains available for moisture absorption changes. At compressive loads, the free volume reduces, forcing the water molecules to move to regions of larger free volume. Thus, the mechanical model and the moisture transport model need to be strongly coupled to simulate the behaviour of PA6. Many authors have modelled this behaviour with the help of a dependency of material parameters on the concentration [3, 18, 19, 21, 26, 30]. There is also an observed change in the viscoelastic relaxation behaviour related to the phase transition caused by the presence of moisture,

Communicated by Marcus Aßmus, Victor A. Eremeyev and Andreas Öchsner.

P. Sharma (✉) · S. Diebels
Chair of Applied Mechanics, Campus A4 2, 66123 Saarbrücken, Germany
E-mail: prateek.sharma@uni-saarland.de

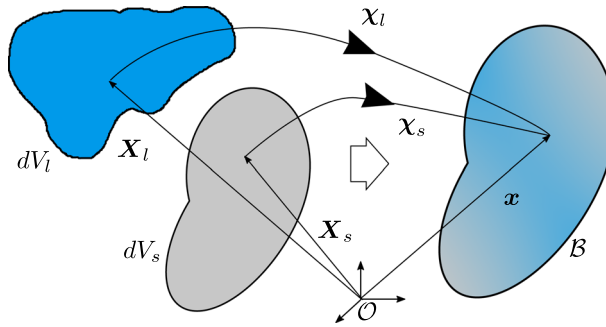


Fig. 1 A mixture of polyamide (solid: s) and moisture (liquid: l) in the current configuration on the right with the mapping to the reference configuration on the left

which has been captured by interpolating the relaxation times between the dry and saturated specimen to an effective relaxation time [19,30]. Further, the coupling of the diffusion model to the mechanical loading has been performed by making the diffusion coefficient a function of the strain values [3,21].

A usual approach for setting the theoretical basis for modelling the coupled behaviour is to treat the two components, i.e. the water and polymer, as two different continua that are volumetrically interacting with each other. The balance equations to describe both the phases can be used to model the mixture using the concept of superimposed continua. A general multiphase mixture has been tackled among others in the works of Truedell and Toupin [31,32], Müller [24], Bowen [8] and Dunwoody [14], and the foundation for the different variations was laid. The concept was extended with the help of volume fractions that led to the development of theory of porous media [5,7]. In more recent works, Diebels included the rotatory degrees of freedom and the micropolar deformations were handled [11,12]. Johlitz utilised the framework to introduce a chemical reaction between the diffusing material and the solid skeleton [19]. He used the Liu–Müller form of entropy evaluation in order to get the constitutive equations for the field quantities. Neff et al. [26] and Villani et al. [33] used this framework to explain the swelling in polymers. Engelhard included the temperature field along with the two-phase model [16]. He also used the Gibb’s free energy instead of the usual Helmholtz energy for the entropy evaluation.

In the present work, the theoretical basis of the mixture theory for two phases is utilised to develop the coupling between the mechanical model and the moisture transport model. An entropy evaluation is conducted to test the consistency of the constitutive equations employed for the strongly coupled model.

2 Mixture kinematics

To model the behaviour of polyamide in the presence of moisture, two different superimposed continua are considered, namely polyamide as a solid phase with the subscript s and moisture as a liquid phase with the subscript l (Fig. 1). The mixture exists only in the current configuration, and hence, both the components follow their respective paths from an individual and arbitrary reference configuration to the current configuration given by $\chi_s(X_s, t)$ and $\chi_l(X_l, t)$, respectively. The current position x is simultaneously occupied by the particles of both the solid phase and the liquid phase

$$x = \chi_s(X_s, t) = \chi_l(X_l, t). \quad (1)$$

The motion of both the components is invertible, and the spatial representation of velocity can be defined as:

$$v_\alpha = \frac{\partial x(\chi_\alpha^{-1}(x, t))}{\partial t}, \quad (2)$$

and the deformation gradient tensor as

$$\mathbf{F}_\alpha = \text{Grad}_\alpha \chi_\alpha \quad (3)$$

for $\alpha = s, l$. The operator ‘Grad $_\alpha$ ’ defines the gradient with respect to (w.r.t) the reference configuration. The displacement for any phase can be calculated by

$$u_\alpha = x - X_\alpha \quad (4)$$

which can be used to write the deformation gradient tensor as

$$\mathbf{F}_\alpha = \mathbf{I} + \text{Grad}_\alpha \mathbf{u}_\alpha. \quad (5)$$

The velocity gradient tensor of the phases is given by

$$\mathbf{L}_\alpha = \text{grad } \mathbf{v}_\alpha = (\mathbf{F}_\alpha)'_\alpha \mathbf{F}_\alpha^{-1} \quad (6)$$

with the operator ‘grad’ represents the gradient w.r.t the current configuration. The velocity gradient tensor can be further split into a symmetric part \mathbf{D}_α and a skew-symmetric part \mathbf{W}_α . The operator $(\cdot)'_\alpha$ represents the material time derivative w.r.t the motion of phase α . The material time derivative for any physical quantity (φ) in space

$$(\varphi)'_\alpha = \frac{\partial \varphi}{\partial t} + \text{grad } \varphi \cdot \mathbf{v}_\alpha, \quad (7)$$

includes the change in the quantity caused by the flow of the component with the velocity \mathbf{v}_α . Apart from the individual phase velocities, the seepage velocity

$$\mathbf{w} = \mathbf{v}_l - \mathbf{v}_s \quad (8)$$

is introduced in order to describe the relative motion of the moisture w.r.t the solid polyamide. Using the seepage velocity, the material time derivative w.r.t the motion of the liquid can be transformed with

$$(\varphi)'_l = (\varphi)'_s + \text{grad } \varphi \cdot \mathbf{w} \quad (9)$$

to a material derivative w.r.t the motion of polyamide. In the following section, the solid polyamide defines the boundary of an open system over which the fluid is flowing in. Thus, the time derivatives of the quantities are rewritten in terms of the solid phase motion using relation (9), and the flow of the fluid phase over the boundary is governed by the seepage velocity (8).

3 Balance equations

A general balance equation of a mass-specific quantity $\rho_s \varphi_s$ for the polyamide is given by [13]

$$(\rho_s \varphi_s)'_s + \rho_s \varphi_s \text{div } \mathbf{v}_s = \text{div } \boldsymbol{\phi}_s + \beta_s + \hat{\phi}_s, \quad (10)$$

with $\boldsymbol{\phi}_s$ being the flow term, β_s the supply term, and $\hat{\phi}_s$ being the production term. The operator ‘div’ is the divergence operator in the current configuration. Similarly, for the moisture, the terms $\boldsymbol{\phi}_l$, β_l , and $\hat{\phi}_l$ give the right-hand side of the balance equation; however, for the left-hand side, the relations (8) and (9) can be used which leads to

$$(\rho_l \varphi_l)'_l + \rho_l \varphi_l \text{div } \mathbf{v}_l = (\rho_l \varphi_l)'_s + \rho_l \varphi_l \text{div} (\rho_l \varphi_l \mathbf{w}) + \rho_l \varphi_l \text{div } \mathbf{v}_s. \quad (11)$$

The general balance equation for the moisture is therefore represented by

$$(\rho_l \varphi_l)'_s + \text{div} (\rho_l \varphi_l \mathbf{w}) + \rho_l \varphi_l \text{div } \mathbf{v}_s = \text{div } \boldsymbol{\phi}_l + \beta_l + \hat{\phi}_l. \quad (12)$$

The balance equation for the mixture is obtained by the summation of the balance equations for the individual components

$$\sum_{\alpha=s,l} ((\rho_\alpha \varphi_\alpha)'_s + \rho_\alpha \varphi_\alpha \text{div } \mathbf{v}_s) + \text{div} (\rho_l \varphi_l \mathbf{w}) = \sum_{\alpha=s,l} (\text{div } \boldsymbol{\phi}_\alpha + \beta_\alpha + \hat{\phi}_\alpha). \quad (13)$$

3.1 Mass balance

The mass balances for the two constituents are given by

$$(\rho_s)'_s + \rho_s \operatorname{div} \mathbf{v}_s = \hat{\rho}_s, \text{ and} \quad (14)$$

$$(\rho_l)'_s + \rho_l \operatorname{div} \mathbf{v}_s + \operatorname{div} (\rho_l \mathbf{w}) = \hat{\rho}_l, \quad (15)$$

where ρ_s and ρ_l denote the partial mixture density of the polyamide and the moisture, respectively. The mass production terms give the transfer of mass from one phase to the other. Since in this work only the physical movement of the moisture is studied and it is assumed that no chemical reactions are taking place, the individual mass production terms can be assumed to be zero, i.e. $\hat{\rho}_s = 0$ and $\hat{\rho}_l = 0$. For the entire mixture, the two mass balances can be added to get

$$(\rho)'_s + \rho \operatorname{div} \mathbf{v}_s + \operatorname{div} (\mathbf{j}) = 0, \quad (16)$$

where the total mass production $\hat{\rho}_s + \hat{\rho}_l = 0$, as there is no mass produced in the mixture and $\rho = \rho_s + \rho_l$ is the density of the mixture. The third term in the mass balance equation for the mixture shows that the mixture does not have a constant mass w.r.t the domain occupied by the solid and it keeps on increasing with the flow of the moisture into the body. Here, $\mathbf{j} = \rho_l \mathbf{w}$ represents the mass flow of the moisture w.r.t the moving solid.

3.2 Momentum balance

For the momentum balance, the physical quantity φ_α should be substituted with the velocity \mathbf{v}_α in the general balance equation to get

$$(\rho_s \mathbf{v}_s)'_s + \rho_s \mathbf{v}_s \operatorname{div} \mathbf{v}_s = \operatorname{div} \mathbf{T}_s + \rho_s \mathbf{b}_s + \hat{\mathbf{P}}_s, \text{ and} \quad (17)$$

$$(\rho_l \mathbf{v}_l)'_s + \operatorname{div} (\rho_l \mathbf{v}_l \otimes \mathbf{w}) + \rho_l \mathbf{v}_l \operatorname{div} \mathbf{v}_s = \operatorname{div} \mathbf{T}_l + \rho_l \mathbf{b}_l + \hat{\mathbf{P}}_l, \quad (18)$$

where \mathbf{T}_s and \mathbf{T}_l are the Cauchy stress tensors, \mathbf{b}_s and \mathbf{b}_l are the body force densities and $\hat{\mathbf{P}}_s$ and $\hat{\mathbf{P}}_l$ are the interaction forces. The summation over the two phases gives the mixture equation

$$(\rho \mathbf{v})'_s + \rho \mathbf{v} \operatorname{div} \mathbf{v}_s + \operatorname{div} (\mathbf{j} \otimes \mathbf{v}_l) = \operatorname{div} (\mathbf{T}_s + \mathbf{T}_l) + \rho \mathbf{b}. \quad (19)$$

Here, $\mathbf{v} = (\rho_s \mathbf{v}_s + \rho_l \mathbf{v}_l) / \rho$ defines the barycentric velocity of the mixture and again the interaction terms add up to zero $\hat{\mathbf{P}}_s + \hat{\mathbf{P}}_l = 0$. The sum of the body forces is given by $\rho \mathbf{b} = \rho_s \mathbf{b}_s + \rho_l \mathbf{b}_l$.

3.3 Energy balance

In order to satisfy the conservation of energy, changes in the internal energy e and the kinetic energy need to be balanced with the heat flow \mathbf{q} and the heat production ρr due to radiation. Hence, based on the general balance equation with $\varphi_\alpha = e_\alpha + \frac{1}{2} \mathbf{v}_\alpha \cdot \mathbf{v}_\alpha$, the energy balance of the polyamide phase becomes

$$\left(\rho_s e_s + \frac{1}{2} \rho_s \mathbf{v}_s \cdot \mathbf{v}_s \right)'_s + \left(\rho_s e_s + \frac{1}{2} \rho_s \mathbf{v}_s \cdot \mathbf{v}_s \right) \operatorname{div} \mathbf{v}_s = \operatorname{div} (\mathbf{T}_s \cdot \mathbf{v}_s) + \rho_s \mathbf{b}_s \cdot \mathbf{v}_s + \rho_s r_s - \operatorname{div} \mathbf{q}_s + \hat{e}_s. \quad (20)$$

After some algebraic manipulation using Eqs. (14) and (17), the energy of the solid phase reads

$$(\rho_s e_s)'_s + \rho_s e_s \operatorname{div} \mathbf{v}_s = \mathbf{T}_s : \mathbf{D}_s + \rho_s r_s - \operatorname{div} \mathbf{q}_s + \hat{e}_s - \mathbf{v}_s \cdot \hat{\mathbf{P}}_s. \quad (21)$$

It is usual in the literature to reduce the left-hand side of the balance equation with the help of the mass balance (14) to

$$\rho_s (e_s)'_s = \mathbf{T}_s : \mathbf{D}_s + \rho_s r_s - \operatorname{div} \mathbf{q}_s - \mathbf{v}_s \cdot \hat{\mathbf{P}}_s + \hat{e}_s. \quad (22)$$

The energy balance equation for the moisture can be written in a similar way

$$\left(\rho_l e_l + \frac{1}{2} \rho_l \mathbf{v}_l \cdot \mathbf{v}_l \right)'_s + \left(\rho_l e_l + \frac{1}{2} \rho_l \mathbf{v}_l \cdot \mathbf{v}_l \right) \operatorname{div} \mathbf{v}_s = \operatorname{div} (\mathbf{T}_l \cdot \mathbf{v}_l) + \rho_l \mathbf{b}_l \cdot \mathbf{v}_l + \rho_l r_l - \operatorname{div} \mathbf{q}_l + \hat{e}_l. \quad (23)$$

Here, the time derivative is again formulated w.r.t the motion of the solid phase. However, when substituting the mass balance (15) and momentum balance (18) in the energy balance of the liquid, extra terms related to the flow of the moisture into the system are obtained

$$(\rho_l e_l)'_s + \rho_l e_l \operatorname{div} \mathbf{v}_s = \mathbf{T}_l : \mathbf{D}_l + \rho_l r_l - \operatorname{div} \mathbf{q}_l + \hat{e}_l - \mathbf{v}_l \cdot \hat{\mathbf{P}}_l - \operatorname{div} (e_l \mathbf{j}). \quad (24)$$

and by further reduction of the left-hand side with the help of Eq. (15)

$$\rho_l (e_l)'_s = \mathbf{T}_l : \mathbf{D}_l + \rho_l r_l - \operatorname{div} \mathbf{q}_l + \hat{e}_l - \mathbf{v}_l \cdot \hat{\mathbf{P}}_l - \operatorname{div} (e_l \mathbf{j}) + e_l \operatorname{div} \mathbf{j} \quad (25)$$

is obtained. By the application of the divergence theorem, the equation can be written as

$$\rho_l (e_l)'_s = \mathbf{T}_l : \mathbf{D}_l + \rho_l r_l - \operatorname{div} \mathbf{q}_l + \hat{e}_l - \mathbf{v}_l \cdot \hat{\mathbf{P}}_l - \operatorname{grad} e_l \cdot \mathbf{j}. \quad (26)$$

For the mixture, Eqs. (21) and (24) are added, yielding

$$\rho(e)'_s = \mathbf{T}_s : \mathbf{D}_s + \mathbf{T}_l : \mathbf{D}_l + (\rho_s r_s + \rho_l r_l) - \operatorname{div} (\mathbf{q}_s + \mathbf{q}_l) - \hat{\mathbf{P}}_l \cdot \mathbf{w} - \operatorname{div} (e_l \mathbf{j}) + e \operatorname{div} \mathbf{j}. \quad (27)$$

Here, $\rho e = \rho_s e_s + \rho_l e_l$ represents the weighted average quantity for the mixture, similar to the barycentric velocity. The term $\operatorname{div} (e_l \mathbf{j})$ is the flow of the internal energy due to the flow of the moisture in the mixture, whereas the term $e \operatorname{div} \mathbf{j}$ is the change in the average internal energy of the mixture due to the change in the ratio of the masses of liquid to the solid driven by the relative motion of the fluid w.r.t the solid.

3.4 Entropy balance

Similar to the energy and momentum balance, the entropy balance for the polyamide follows the general balance equation formulation and results in

$$(\rho_s \eta_s)'_s + \rho_s \eta_s \operatorname{div} \mathbf{v}_s = -\operatorname{div} \left(\frac{\mathbf{q}_s}{\theta} \right) + \frac{\rho_s r_s}{\theta} + \hat{\eta}_s \quad (28)$$

or

$$\rho_s (\eta_s)'_s = -\operatorname{div} \left(\frac{\mathbf{q}_s}{\theta} \right) + \frac{\rho_s r_s}{\theta} + \hat{\eta}_s. \quad (29)$$

The specific entropy of the polyamide phase is represented by η_s which is at a temperature θ . Since the process of moisture transport is slow, it can be assumed that the temperatures of both the constituents equalise and $\theta = \theta_s = \theta_l$ can be substituted in the entropy balances. For the moisture along with the supply and production term, the flow term also causes a change in the entropy which is given by

$$(\rho_l \eta_l)'_s + \rho_l \eta_l \operatorname{div} \mathbf{v}_s = -\operatorname{div} \left(\frac{\mathbf{q}_l}{\theta} \right) + \frac{\rho_l r_l}{\theta} + \hat{\eta}_l - \operatorname{div} (\eta_l \mathbf{j}). \quad (30)$$

By using the mass balance equation for the moisture (15),

$$\rho_l (\eta_l)'_s = -\operatorname{div} \left(\frac{\mathbf{q}_l}{\theta} \right) + \frac{\rho_l r_l}{\theta} + \hat{\eta}_l - \mathbf{j} \cdot \operatorname{grad} \eta_l \quad (31)$$

is obtained.

4 Entropy evaluation

The unknowns of the mixture can be determined when the mass balance (14), (15) and the momentum balance (19) are solved. The momentum balance for the mixture is solved instead of the individual phases as the relative momentum change between the phases is negligible. Moreover, the mass of the solid remains constant. Therefore, the constitutive quantities

$$\mathcal{R} = \{\mathbf{T}_s, \mathbf{T}_l, \mathbf{j}\} \quad (32)$$

need to be chosen in a thermodynamically consistent way to solve the balance equations. To this end, the entropy balances of the individual constituents are transformed using the Legendre transformation

$$\psi_\alpha = e_\alpha - \eta_\alpha \theta \quad (33)$$

where ψ_α denotes the Helmholtz energy for phase $\alpha = s, l$. For an isothermal process where the change of temperature w.r.t time is zero, the transformation of Eqs. (29) and (31) yields

$$-\rho_s(\psi_s)'_s + \mathbf{T}_s : \mathbf{D}_s - \mathbf{v}_s \cdot \hat{\mathbf{P}}_s + \hat{e}_s = \hat{\eta}_s \quad (34)$$

for the polyamide and

$$-\rho_l(\psi_l)'_s + \mathbf{T}_l : \mathbf{D}_l - \mathbf{v}_l \cdot \hat{\mathbf{P}}_l - \mathbf{j} \cdot \text{grad } \psi_l + \hat{e}_l = \hat{\eta}_l \quad (35)$$

for the moisture. According to the second law of thermodynamics in a viable process, the entropy of the system must not decrease. Hence, $\hat{\eta} = \hat{\eta}_s + \hat{\eta}_l$ should always be non-negative. By the addition of Eq. (34) and Eq. (35), and by employing the inequality $\hat{\eta}_s + \hat{\eta}_l \geq 0$, the Clausius–Planck inequality

$$-\rho_s(\psi_s)'_s - \rho_l(\psi_l)'_s + \mathbf{T}_s : \mathbf{D}_s + \mathbf{T}_l : \mathbf{D}_l - \mathbf{w} \cdot \hat{\mathbf{P}}_l - \mathbf{j} \cdot \text{grad } \psi_l \geq 0 \quad (36)$$

is obtained. The relation (36) is evaluated for the thermodynamic consistency using the Liu–Müller method [23,24]. The mass balance and the momentum balance for the moisture are added to the entropy Eq. (36) with the help of Lagrangian parameters Λ_1 and Λ_2 , respectively,

$$\begin{aligned} & -\rho_s(\psi_s)'_s - \rho_l(\psi_l)'_s + \mathbf{T}_s : \mathbf{D}_s + \mathbf{T}_l : \mathbf{D}_l - \mathbf{w} \cdot \hat{\mathbf{P}}_l - \mathbf{j} \cdot \text{grad } \psi_l \\ & + \Lambda_1((\rho_l)'_s + \text{div } \mathbf{j} + \rho_l \text{div } \mathbf{v}_s) \\ & + \Lambda_2 \cdot (\rho_l(\mathbf{v}_l)'_s - \rho_l \mathbf{b}_l - \mathbf{v}_l \text{div } \mathbf{j} + \text{div } (\mathbf{j} \otimes \mathbf{v}_s) - \text{div } \mathbf{T}_l - \hat{\mathbf{P}}_l) \geq 0. \end{aligned} \quad (37)$$

As the process is quasi-static both in terms of the mechanical deformation and the moisture transport, the inertial terms in the momentum balance equation are neglected. Thus, the entropy inequality with the modified momentum balance equation can be rewritten as:

$$\begin{aligned} & -\rho_s(\psi_s)'_s - \rho_l(\psi_l)'_s + \mathbf{T}_s : (\boldsymbol{\epsilon})'_s + \mathbf{T}_l : \mathbf{D}_l - \mathbf{w} \cdot \hat{\mathbf{P}}_l - \mathbf{j} \cdot \text{grad } \psi_l \\ & + \Lambda_1((\rho_l)'_s + \mathbf{w} \cdot \text{grad } \rho_l + \rho_l \text{div } \mathbf{v}_l) \\ & + \Lambda_2 \cdot (-\text{div } \mathbf{T}_l - \hat{\mathbf{P}}_l) \geq 0. \end{aligned} \quad (38)$$

For simplicity, the model is developed for small deformations, and a geometrically linear deformation is assumed. To this end, the strain is formulated as the symmetric part of the displacement gradient

$$\boldsymbol{\epsilon}_s = \frac{\text{grad } \mathbf{u}_s + \text{grad}^T \mathbf{u}_s}{2} \quad (39)$$

and $\mathbf{D}_s = (\boldsymbol{\epsilon}_s)'_s$ is assumed. Furthermore, the strain is split additively into an elastic and an inelastic part

$$\boldsymbol{\epsilon}_s = \boldsymbol{\epsilon}_e + \boldsymbol{\epsilon}_i \quad (40)$$

to account for the viscoelastic behaviour of the polymer [20,28]. The deformation of the solid part is thus related to the variables $\boldsymbol{\epsilon}_s, \boldsymbol{\epsilon}_i$. The fluid deformation is defined by the deformation velocity given by \mathbf{D}_l . The mass flow of the phases is modelled with the variables ρ_s, ρ_l and the gradient of the densities $\text{grad } \rho_s$ and $\text{grad } \rho_l$. Thus, the set of process variables for the linear viscoelastic solid interacting with the diffusion process at a constant temperature is chosen as [11,20]

$$\mathcal{S} = (\boldsymbol{\epsilon}_s, \boldsymbol{\epsilon}_i, \mathbf{D}_l, \rho_s, \rho_l, \text{grad } \rho_s, \text{grad } \rho_l). \quad (41)$$

The free energy functions depend only on the process variables

$$\psi_{s,l} = \psi_{s,l}(\mathcal{S}). \quad (42)$$

The principle of equipresence is assumed, and therefore, all material time derivatives can be written as:

$$(\psi_{s,l}(\mathcal{S}))'_s = \frac{\partial \psi_{s,l}}{\partial \mathcal{S}} (\mathcal{S})'_s \quad (43)$$

using the chain rule of differentiation. Substituting the derivative in the inequality (38) and rearranging the terms lead to

$$\begin{aligned} (\boldsymbol{\epsilon}_s)'_s : & \left[-\rho_s \frac{\partial \psi_s}{\partial \boldsymbol{\epsilon}_s} - \rho_l \frac{\partial \psi_l}{\partial \boldsymbol{\epsilon}_s} + \mathbf{T}_s \right] + (\mathbf{D}_l)'_s : \left[-\rho_s \frac{\partial \psi_s}{\partial \mathbf{D}_l} - \rho_l \frac{\partial \psi_l}{\partial \mathbf{D}_l} \right] \\ & + (\rho_s)'_s \left[-\rho_s \frac{\partial \psi_s}{\partial \rho_s} - \rho_l \frac{\partial \psi_l}{\partial \rho_s} \right] + (\rho_l)'_s \left[-\rho_s \frac{\partial \psi_s}{\partial \rho_l} - \rho_l \frac{\partial \psi_l}{\partial \rho_l} + \Lambda_1 \right] \\ & + (\text{grad } \rho_s)'_s \cdot \left[-\rho_s \frac{\partial \psi_s}{\partial \text{grad } \rho_s} - \rho_l \frac{\partial \psi_l}{\partial \text{grad } \rho_s} \right] \\ & + (\text{grad } \rho_l)'_s \cdot \left[-\rho_s \frac{\partial \psi_s}{\partial \text{grad } \rho_l} - \rho_l \frac{\partial \psi_l}{\partial \text{grad } \rho_l} \right] \\ & + \mathcal{D} \geq 0 \end{aligned} \quad (44)$$

with the residual inequality

$$\begin{aligned} \mathcal{D} = (\boldsymbol{\epsilon}_i)'_s : & \left[-\rho_s \frac{\partial \psi_s}{\partial \boldsymbol{\epsilon}_i} - \rho_l \frac{\partial \psi_l}{\partial \boldsymbol{\epsilon}_i} \right] - \hat{\mathbf{P}}_l \cdot (\mathbf{w} + \boldsymbol{\Lambda}_2) - \mathbf{j} \cdot \text{grad } \psi_l \\ & - \boldsymbol{\Lambda}_2 \cdot \text{grad } p_l + \mathbf{D}_l : (-p_l \mathbf{I} + \rho_l \Lambda_1 \mathbf{I}) + \Lambda_1 \mathbf{w} \cdot \text{grad } \rho_l. \end{aligned} \quad (45)$$

While frictional effects in the fluid mainly govern the momentum exchange $\hat{\mathbf{P}}_s = -\hat{\mathbf{P}}_l$ [15], the stress in the moisture can be assumed to be hydrostatic and hence has been transformed to $\mathbf{T}_l = -p_l \mathbf{I}$ with p_l being the hydrostatic pore pressure. Following the arguments of entropy evaluation and using the fact that the rate of change of the process variables can be arbitrary, the following relationships are obtained as necessary and sufficient conditions [23,24]:

$$-\rho_s \frac{\partial \psi_s}{\partial \mathbf{D}_l} - \rho_l \frac{\partial \psi_l}{\partial \mathbf{D}_l} = 0, \quad (46)$$

$$-\rho_s \frac{\partial \psi_s}{\partial \rho_s} - \rho_l \frac{\partial \psi_l}{\partial \rho_s} = 0, \quad (47)$$

$$-\rho_s \frac{\partial \psi_s}{\partial \text{grad } \rho_s} - \rho_l \frac{\partial \psi_l}{\partial \text{grad } \rho_s} = 0, \quad (48)$$

$$-\rho_s \frac{\partial \psi_s}{\partial \text{grad } \rho_l} - \rho_l \frac{\partial \psi_l}{\partial \text{grad } \rho_l} = 0, \quad (49)$$

$$\Lambda_1 = \rho_s \frac{\partial \psi_s}{\partial \rho_l} + \rho_l \frac{\partial \psi_l}{\partial \rho_l}, \quad (50)$$

$$\mathbf{T}_s = \rho_s \frac{\partial \psi_s}{\partial \boldsymbol{\epsilon}_s} + \rho_l \frac{\partial \psi_l}{\partial \boldsymbol{\epsilon}_s}. \quad (51)$$

The first term of the residual inequality (45) contains the derivative of the inelastic strain. The evolution of the inelastic strain $(\boldsymbol{\epsilon}_i)'_s$ should not be arbitrary as it is an internal variable that depends on the relaxation time of the polyamide. Thus, an evolution equation is employed which ensures that

$$(\boldsymbol{\epsilon}_i)'_s : \left[-\rho_s \frac{\partial \psi_s}{\partial \boldsymbol{\epsilon}_i} - \rho_l \frac{\partial \psi_l}{\partial \boldsymbol{\epsilon}_i} \right] \geq 0 \quad (52)$$

is satisfied which is sufficient to fulfil the respective part of the residual inequality. The interaction force $\hat{\mathbf{P}}_l$ between the polyamide and the moisture is generating a flow. The momentum balance of the liquid phase is

not solved explicitly to determine \mathbf{j} , rather \mathbf{j} is defined as a constitutive quantity. Hence, the interaction force is not included in the set of constitutive variables (32) and any value of $\hat{\mathbf{P}}_l$ should fulfil the residual inequality, which can be ensured by the choice

$$\mathbf{\Lambda}_2 = -\mathbf{w}, \quad (53)$$

making the term disappear in Eq. (45). The remaining inequality becomes

$$\mathcal{D} = -\mathbf{j} \cdot \text{grad } \psi_l - \mathbf{w} \cdot \text{grad } p_l + \mathbf{D}_l : (-p_l \mathbf{I} + \rho_l \Lambda_1 \mathbf{I}) + \Lambda_1 \mathbf{w} \cdot \text{grad } \rho_l \geq 0. \quad (54)$$

Here, the chemical potential for the liquid [8, 14, 22, 32]

$$\kappa_l = \psi_l - \frac{p_l}{\rho_l} \quad (55)$$

is introduced and substituted in \mathcal{D} . In this way, the Helmholtz free energy for the solid and the chemical potential for the liquid define the two potentials for the coupled problem. Equation (54) is transformed with the help of these potentials to

$$-\mathbf{j} \cdot \text{grad } \kappa_l + \mathbf{D}_l : (-p_l \mathbf{I} + \rho_l \Lambda_1 \mathbf{I}) - \left(-\frac{p_l \mathbf{j}}{\rho_l^2} + \Lambda_1 \mathbf{w} \right) \cdot \text{grad } \rho_l \geq 0. \quad (56)$$

The inequality should not be harmed for any deformation velocity of the liquid, therefore

$$p_l = \rho_l \Lambda_1, \quad (57)$$

and by using Eq. (50)

$$p_l = \rho_l \rho_s \frac{\partial \psi_s}{\partial \rho_s} + \rho_l^2 \frac{\partial \psi_l}{\partial \rho_l} \quad (58)$$

is obtained. The residual inequality reduces to

$$-\mathbf{j} \cdot \text{grad } \kappa_l \geq 0. \quad (59)$$

The inequality can be satisfied if

$$\mathbf{j} = -k (\text{grad } \kappa_l), \quad (60)$$

where $k \geq 0$ is a material parameter which has the character of a diffusion constant. Thus, the conditions for the constitutive quantities are obtained, which are exploited to get the equations of these quantities in the next section.

5 Constitutive equation

A set of constitutive equations needs to be chosen, to describe the physical properties of polyamide and its absorption mechanism. According to the physical process observed in experiments [30], the process variables are split between the two potentials

$$\begin{aligned} \psi_s &= \psi_s(\mathbf{e}_s, \mathbf{e}_i, \rho_l) \\ \kappa_l &= \kappa_l(\rho_l). \end{aligned} \quad (61)$$

It was observed for polyamide that the mass uptake is proportional to the square root of time, which indicates a Fick's model of diffusion. Here, the moisture mass concentration w.r.t the dry solid

$$c = \frac{\rho_l}{\rho_s} \quad (62)$$

is introduced. Substituting the definition of concentration in the mass balance equation for the moisture (15) results in

$$\rho_s (c)'_s + \text{div } \mathbf{j} = 0, \quad (63)$$

which is similar to the Fick's diffusion model. Therefore, considering the Fickian behaviour and the dependency of the moisture flow on the pressure, the chemical potential is given by

$$\kappa_l = D \rho_l + K p_l \quad (64)$$

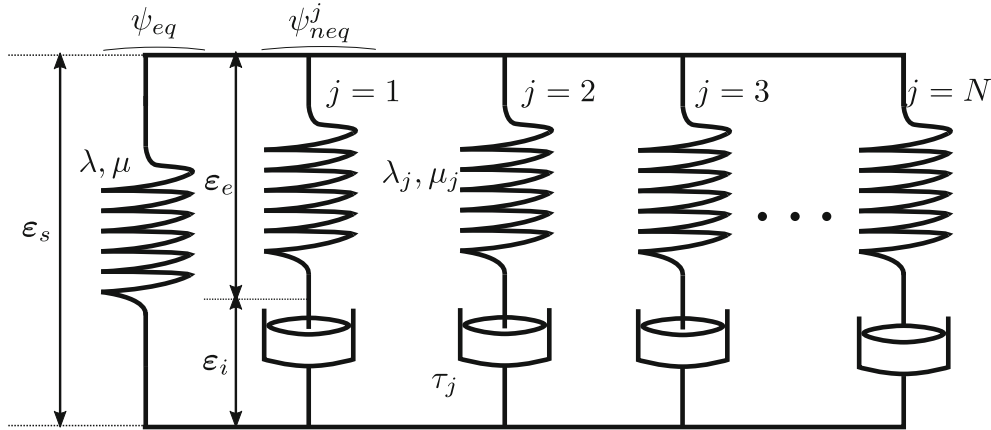


Fig. 2 The rheological model to represent the viscoelastic behaviour

similar to the chemical potential taken by Villani et al. [33] and Sar et al. [29]. Thus, combining Eqs. (64), (60) and (63), the following expression

$$\rho_s(c)'_s = \text{div}(D \text{grad}(\rho_s c) + K \text{grad} p_l) \quad (65)$$

is obtained. Using the ideal gas equation, the liquid pressure is calculated with the help of a linear relationship between the density and the pressure

$$p_l = R\theta\rho_l = R\theta c\rho_s \quad (66)$$

where R is the ideal gas constant. Note that the temperature θ was assumed to be constant.

The mechanical behaviour of polyamide is viscoelastic in nature and is modelled with a rheological model with N Maxwell elements (Fig. 2).

The free energy is calculated with the strain energy induced in the springs of the rheological elements. The element without the dashpot represents the equilibrium part, and its free energy depends on the strain $\mathbf{\epsilon}_s$, whereas the free energy of the Maxwell elements depends on the elastic part of the strain $\mathbf{\epsilon}_e = \mathbf{\epsilon}_s - \mathbf{\epsilon}_i$. This can be represented as

$$\Psi_s = \Psi_{seq}(\mathbf{\epsilon}_s) + \Psi_{sneq}(\mathbf{\epsilon}_s - \mathbf{\epsilon}_i). \quad (67)$$

With the Lamé parameters μ and λ

$$\begin{aligned} \rho_s \Psi_{seq} &= \left(\mu(c) \mathbf{\epsilon}_s : \mathbf{\epsilon}_s + \frac{\lambda(c)}{2} \text{tr}(\mathbf{\epsilon}_s)^2 \right), \\ \rho_s \Psi_{sneq}^j &= \left(\mu_j(c) (\mathbf{\epsilon}_s - \mathbf{\epsilon}_i^j) : (\mathbf{\epsilon}_s - \mathbf{\epsilon}_i^j) + \frac{\lambda_j(c)}{2} \text{tr}(\mathbf{\epsilon}_s - \mathbf{\epsilon}_i^j)^2 \right) \end{aligned} \quad (68)$$

give the equilibrium and the non-equilibrium part of the free energy, respectively. With this, the stress in the polyamide is given by

$$\mathbf{T}_s = \rho_s \frac{\partial \Psi_s}{\partial \mathbf{\epsilon}_s} = 2\mu(c)\mathbf{\epsilon}_s + \lambda(c)\text{tr}(\mathbf{\epsilon}_s)\mathbf{I} + \sum_{j=0}^N \left(2\mu_j(c)(\mathbf{\epsilon}_s - \mathbf{\epsilon}_i^j) + \lambda_j(c)\text{tr}(\mathbf{\epsilon}_s - \mathbf{\epsilon}_i^j)\mathbf{I} \right). \quad (69)$$

The evolution equation for the inelastic part is taken in a standard way by

$$\left(\mathbf{\epsilon}_i^j \right)'_s = \frac{\mathbf{\epsilon}_s - \mathbf{\epsilon}_i^j}{\tau^j/2}, \quad (70)$$

where τ^j represents the relaxation time for the j th Maxwell element. The Lamé parameters vary with the moisture concentration

$$\begin{aligned} \lambda(c) &= g(c)\lambda_o \\ \mu(c) &= g(c)\mu_o \end{aligned} \quad (71)$$

and a function $g(c)$ is used to interpolate the parameter for a given moisture concentration c [30]. Typically, a linear or sigmoid interpolation is chosen for $g(c)$.

6 Numerical example

A combination of the momentum balance (19), the mass balance for the moisture (65) and the pressure equation (66)

$$\begin{aligned} \operatorname{div}(\mathbf{T}_s - p_l \mathbf{I}) &= 0 \\ \rho_s(c)'_s &= \operatorname{div}(D \operatorname{grad}(\rho_s c) + K \operatorname{grad} p_l) \\ p_l &= R\theta c \rho_s \end{aligned} \quad (72)$$

serves the basis for the finite element (FE) implementation of the model. The three solution fields, namely the displacement \mathbf{u} , the concentration c and the liquid pressure p_l , are modelled on the element.

$$U = \{\mathbf{u}, c, p_l\} \quad (73)$$

To guarantee the stability of the FE system, the shape function for the displacement field and for the concentration is quadratic in space, whereas it is linear in space for pressure. It should be noted that the moisture transport has a dependency on the gradient of the concentration as well as the gradient of the pressure. The pressure in turn is dependent on the volumetric part of the strain, which is a function of the gradient of the displacement field. Hence, higher-order gradients are incorporated in the moisture transport model. This reflects the gradient character of the presented theory. The density of the solid changes with an applied load, and hence, the loading induces a moisture transport. However, when no loading is applied, then the moisture transport is solely driven by the concentration gradient and hence, the moisture transport equation reduces to

$$(c)'_s = \operatorname{div}(D(c) \operatorname{grad} c). \quad (74)$$

As discussed in [30], the diffusion coefficient is increasing linearly with the increasing concentration, i.e. $D(c) = D_o + D_c c$. Equation (74) is hence a nonlinear diffusion model. However, with the loading, the density of the solid changes according to the relation

$$\rho_s = \rho_{s0} \mathbf{J}^{-1} \quad (75)$$

where \mathbf{J} is the Jacobian and ρ_{s0} is the density of undeformed polyamide. In the case of small deformation, the volumetric strain

$$\varepsilon_{vol} = \operatorname{tr}(\boldsymbol{\varepsilon})/3. \quad (76)$$

and the Jacobian are related according to

$$\mathbf{J} = 1 + \varepsilon_{vol} \quad (77)$$

and the inverse Jacobian can be approximated as

$$\mathbf{J}^{-1} = 1 - \varepsilon_{vol}. \quad (78)$$

Hence, using (78), the moisture transport equation for a specimen subjected to loading can be written as

$$\rho_{s0} \mathbf{J}^{-1} (c)'_s = \operatorname{div}(D(c) \operatorname{grad}(\rho_{s0} \mathbf{J}^{-1} c) + K \operatorname{grad} p_l) \quad (79)$$

and the pressure can be given by

$$p_l = R\theta c \rho_{s0} \mathbf{J}^{-1}. \quad (80)$$

The moisture transport is thus governed by three factors, namely the gradient of the moisture concentration, the gradient of the density of solid, and the gradient of the liquid pressure. The gradient of the concentration drives the Fickian moisture uptake behaviour. Secondly, the compression of solid results in squeezing the moisture, whereas an expansion leads to more affinity for the moisture. Lastly, the pressure gradient drives the flow from the region of high pressure to the region of low pressure. However, for the case considered, the pressure is a linear function of the concentration; hence, some algebraic manipulations of these two equations give

$$\rho_{s0} \mathbf{J}^{-1} (c)'_s = \operatorname{div} \left(\left(\frac{D(c)}{R\theta} + K \right) \operatorname{grad} p_l \right) \quad (81)$$

and the three driving forces are modelled with a single gradient. This equation along with equation (80) and equation (72₁) is solved for a three-point bending test. The coupled system of equations is solved with the help of the Newton's method. The FE model was implemented in the open-source library of deal.II [4].

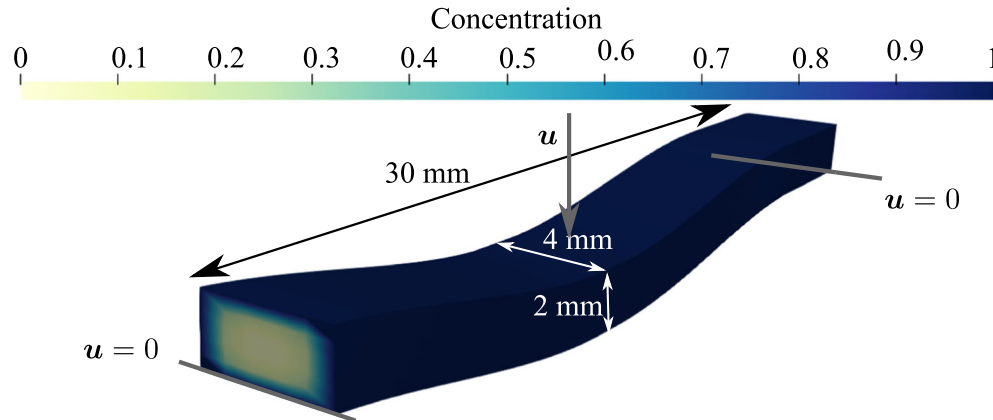


Fig. 3 Three point bending experiment with the supports 30 mm apart. The load is applied on the 4 mm wide face, so the concentration gradient along the 2 mm edge is more dominant

6.1 Geometry and boundary conditions

The geometry and the boundary condition were chosen according to the bending experiment conducted at LKT, TU Dortmund. A specimen of the size 40 mm \times 4 mm \times 2 mm was subjected to three-point bending. The specimen was initially stored in water and regularly measured for the change in its weight. After the specimen had gained 5% of its dry weight, it was taken out of the water and subjected to loading at room temperature and humidity. The maximum concentration or the saturation concentration for a polyamide specimen kept in water was found to be 10% [30]. Therefore, for 5% average concentration, the distribution of moisture within the specimen was inhomogeneous. The specimen with inhomogeneous moisture distribution was placed on two supports that were 30 mm apart from each other. A displacement-driven loading was applied on the specimen exactly in the middle of these two supports. The beam was deflected until 100% of the thickness (2 mm) at 1 mm/min. A deflection of 2 mm was chosen as it results in a maximum strain of 2% in the specimen, which is the limit for the linear viscoelastic model. For more than 2% strain, plastic deformation was seen in tensile tests [30]. The deflection was applied on the 4 mm wide face. In this way, the concentration gradient on the specimen along the 2-mm edge was more dominant in influencing the bending stiffness than the gradient across the 4 mm length (Fig. 3). Numerically, the average concentration of 5% was achieved by applying a normalised saturation concentration of one at all the boundary faces. A starting value for the pressure at the boundary was given according to the equation (80). The displacements at the two supports were constrained to zero, and a displacement u was applied at 1 mm/min after the 5% average concentration was achieved.

6.2 Parameters

The mechanical model parameter were chosen based on the findings in [30]. $N = 4$ Maxwell elements with fixed relaxation times were used to model the viscoelastic behaviour. The moisture transport parameters were, however, determined from the experimental results of the bending experiment. The force versus deflection curves from the experiments were compared with the simulation results, and the Nelder–Mead simplex algorithm was used to minimise the difference between the two sets of curves. Parameters such as $R\theta$ were fixed a priori with their usual values of ideal gas constant and room temperature. Similarly, the density of undeformed solid ρ_{s0} was also taken from the literature [27]. The parameters are summarised in Tables 1 and 2.

6.3 Results

The result of the simulation using the fully coupled model is compared to the solution of a one-way coupled model, where the mechanical response of the material is dependent on the concentration, but the moisture transport is independent of loading (19 and 74). The load versus deflection curve for the bending experiment is shown in Fig. 4a. The fully coupled model results in higher forces as compared to the one-way coupled model. This is attributed to the moisture redistribution within the specimen because of loading (Fig. 5). The moisture

Table 1 Lamé parameter λ for all Maxwell elements for dry ($c = 0$) and saturated material ($c = 1$). Since the Poisson's ratio for the material is unaffected from the moisture content, only λ is listed and μ can be calculated with the Poisson's ratio determined through experiments [30]

Mechanical Parameters					
Maxwell element (j)	basic elasticity	$j = 1$	$j = 2$	$j = 3$	$j = 4$
Relaxation time [s]		0.5	5	50	500
Lamé Parameter (λ_{dry}) Dry [MPa]	1901.93	0	399.2	0.72	1.24
Lamé Parameter (λ_{wet}) Saturated [MPa]	270.83	359.03	446.61	172.41	0

Table 2 The parameters for the moisture transport model

Moisture Transport Parameters					
D_o [mm^2/s]	D_c [mm^2/s]	K [$\text{N mm}^3/\text{g s}$]	$R\theta$ [Nmm/g]	ρ_{so} [g/mm^3]	
1×10^{-13}	5×10^{-13}	1×10^{-7}	1×10^5	1.1×10^{-3}	

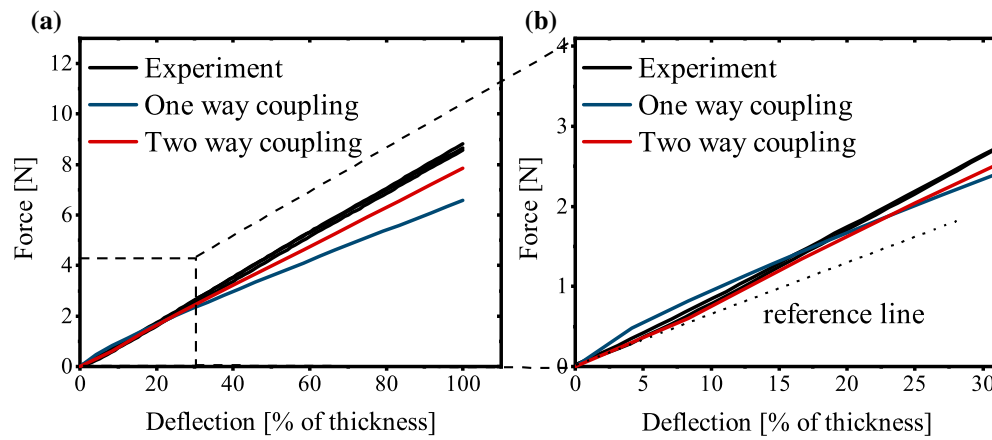


Fig. 4 **a** A comparison of the simulation result for bending with the one-way coupled model, the two-way coupled model and the experimental results from LKT, TU Dortmund. **b** The initial part of the bending shows an upward bend in the curve when compared to the reference line. The upward curves denote the stiffening of the specimen due to the moisture redistribution

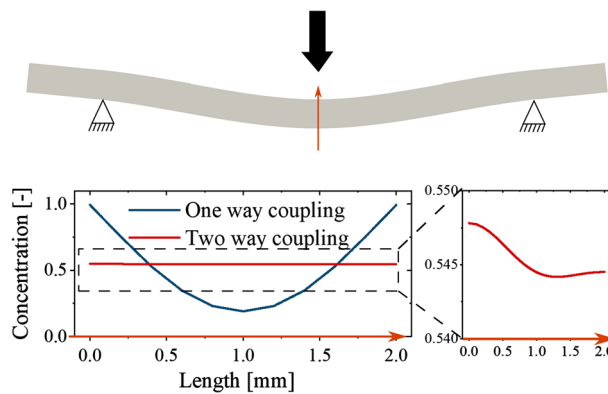


Fig. 5 The concentration profile at the middle of the specimen at the point of loading for the maximum deflection of 2 mm

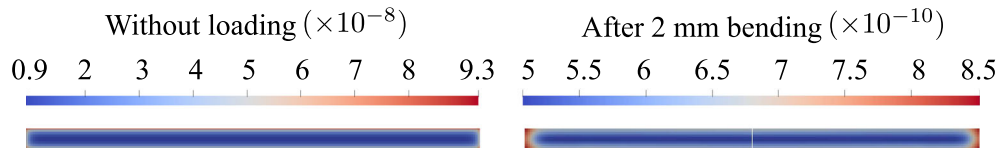


Fig. 6 The distribution of chemical potential before loading on the left and after 2 mm of bending on the right

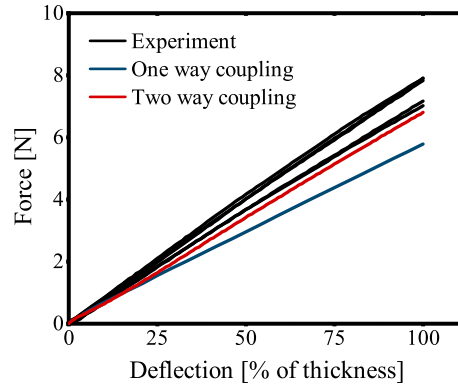


Fig. 7 Comparison of the simulation result with the experimental result at 0.1 mm/min bending rate for 5% average concentration. The two-way coupled model shows a better fit than the one-way coupled model

flows from the top and bottom layer of the specimen towards the centre (from the position of 0 mm and 2 mm to 1 mm in Fig. 5). This can also be understood from the distribution of the chemical potential in (Fig. 6), which shows that the chemical potential drives the moisture transport from the boundary of the specimen towards the middle and towards the ends. Moreover, the bottom layer (at 0 mm in Fig. 5) is in tensile state and has lesser density of the solid which leads to a suction effect and hence higher concentration as compared to the top layer. The fluctuation in the concentration is, however, very small because it is calculated as the ratio of the density of moisture to the density of solid. The increase in moisture density is compensated by the decrease in the solid density to reduce the fluctuation in concentration values. The effect of the redistribution is a higher effective stiffness of the beam and a decrease in the relaxation time. Hence, the two-way coupled model behaves not only stiffer than the one-way coupled model but also more linear, as the viscoelastic relaxation during the loading happens more slowly. The effect of the redistribution is also visible in the experimental result. At the beginning of the loading, an upward curve or a stiffening of the specimen can be seen in the load versus deflection results (Fig. 4b). This stiffening is also noticeable in the two-way coupled model. Thus, the fully coupled model can represent the experimental results more accurately as compared to the one-way coupled model.

The parameters determined with this experiment are used to compare the results for different rate and saturation condition. In Fig. 7, the experimental result for a slower deflection rate of 0.1 mm/min is compared with the simulation result. Here, also the simulation with the two-way coupled model shows a better fit in comparison with the one-way coupled model. It can also be seen that there is a larger difference between the results of the two models. The slower rate allows more time for the moisture redistribution, and hence, the two-way coupled model shows a stiffer material response as compared to the one-way coupled model. Specimens with 10% average concentration or fully saturated specimen were subjected to the bending experiment for both the 1 mm/min and 0.1 mm/min bending rate. The simulation results for these conditions compare well with the experimental results as well (Fig. 8).

7 Conclusion

A theoretical basis for a two-way coupled model is presented using the concept of superimposed continua. A solid or polyamide phase is superimposed on the moisture or the liquid phase. The balance equations are formulated, and the first and second law of thermodynamics are evaluated to define the admissible constitutive equations. The flow of the moisture is found to be dependent on the gradient of the chemical potential. A potential with a linear dependency on the density of liquid and the liquid pressure is chosen. Concentration

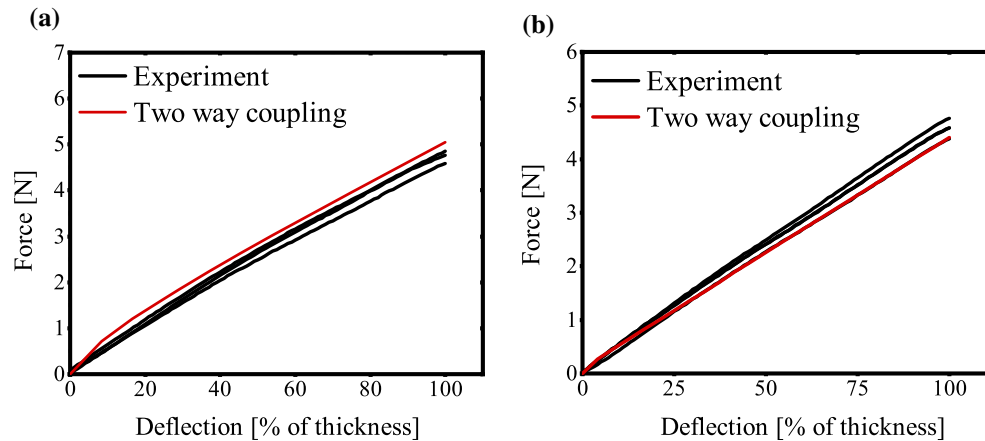


Fig. 8 The force versus deflection results for a fully saturated specimen with 10% average concentration at (a) 1 mm/min and (b) 0.1 mm/min

which is a ratio of the density of the liquid to that of a solid represents the moisture content. As the concentration is a function of the volumetric deformation of the solid phase, the moisture transport model shows a gradient nature. It should be noted that the chemical potential is chosen in a phenomenological way, depending on gravimetric experiments conducted for certain atmospheric condition. However, a more thorough experimental investigation should be conducted to derive the absorption behaviour at different pressures and saturation concentrations for a more fitting selection of the chemical potential. A linear viscoelastic model is used to describe the mechanical behaviour. A numerical example is presented where a one-way coupled model and the fully coupled model are compared. The effect of loading on the moisture redistribution in the specimen and hence the mechanical response of the material is observable in the two-way coupled model. The coupling of the moisture transport to the loading behaviour, results in a stiffening of the specimen and a reduction in the relaxation time which was also observed in the experiment. The fully coupled model can thus predict the experimental results more accurately than the one-way coupled model. Hence, the presented formulation serves as the basis for a thermodynamically consistent model that is valid for the moisture uptake behaviour in polyamides.

Acknowledgements The financial support by the Deutsche Forschungsgemeinschaft DFG under the grant DI 430/29-1 is gratefully acknowledged.

Funding Open Access funding enabled and organized by Projekt DEAL. The funding was provided by the Deutsche Forschungsgemeinschaft DFG under the grant DI 430/29-1.

Open Access This article is licensed under a Creative Commons Attribution 4.0 International License, which permits use, sharing, adaptation, distribution and reproduction in any medium or format, as long as you give appropriate credit to the original author(s) and the source, provide a link to the Creative Commons licence, and indicate if changes were made. The images or other third party material in this article are included in the article's Creative Commons licence, unless indicated otherwise in a credit line to the material. If material is not included in the article's Creative Commons licence and your intended use is not permitted by statutory regulation or exceeds the permitted use, you will need to obtain permission directly from the copyright holder. To view a copy of this licence, visit <http://creativecommons.org/licenses/by/4.0/>.

Declarations

Conflict of interest: The authors declare that they have no conflict of interest.

Availability of data and material: The authors are willing to share the data used for the work.

Code availability: The authors are willing to share the code used to implement the material model.

References

1. Abacha, N., Kubouchi, M., Sakai, T.: Diffusion behavior of water in polyamide 6 organoclay nanocomposites. *Express Polym. Lett.* 3(4), 245–255 (2009)

2. Arhant, M., Le Gac, P.Y., Le Gall, M., Burtin, C., Briançon, C., Davies, P.: Modelling the non Fickian water absorption in polyamide 6. *Polym. Degrad. Stab.* **133**, 404–412 (2016). <https://doi.org/10.1016/j.polymdegradstab.2016.09.001>
3. Bailakanavar, M., Fish, J., Aitharaju, V., Rodgers, W.: Computational coupling of moisture diffusion and mechanical deformation in polymer matrix composites. *Int. J. Numer. Methods Eng.* **98**(12), 859–880 (2014). <https://doi.org/10.1002/nme.4654>
4. Bangerth, W., Hartmann, R., Kanschä, G.: Deal.II - a general purpose object oriented finite element library. *ACM Trans. Math. Softw.* **33**, 24/1-24/27 (2007)
5. de Boer, R., Ehlers, W.: Theorie der Mehrkomponentenkontinua mit Anwendung auf bodenmechanische Problem. Universität - Gesamthochschule - Essen, Essen, Tech. rep. (1986)
6. Boukal, I.: Effect of water on the mechanism of deformation of nylon 6. *J. Appl. Polym. Sci.* **11**(8), 1483–1494 (1967). <https://doi.org/10.1002/app.1967.070110811>
7. Bowen, R.M.: Incompressible porous media models by use of the theory of mixtures. *Int. J. Eng. Sci.* **18**(9), 1129–1148 (1980). [https://doi.org/10.1016/0020-7225\(80\)90114-7](https://doi.org/10.1016/0020-7225(80)90114-7)
8. Bowen, R.M., Wiese, J.C.: Diffusion in mixtures of elastic materials. *Int. J. Eng. Sci.* **7**(7), 689–722 (1969). [https://doi.org/10.1016/0020-7225\(69\)90048-2](https://doi.org/10.1016/0020-7225(69)90048-2)
9. Buchdahl, R., Zaukelies, D.A.: Deformationsprozesse und die Struktur von Kristallinen Polymeren. *Angew. Chem.* **74**(15), 569–573 (1962)
10. Carrascal, I., Casado, J.A., Polanco, J.A., Gutiérrez-Solana, F.: Absorption and diffusion of humidity in fiberglass-reinforced polyamide. *Polym. Compos.* **26**(5), 580–586 (2005). <https://doi.org/10.1002/pc.20134>
11. Diebels, S.: A micropolar theory of porous media: constitutive modelling. *Transp. Porous Media* **34**(1/3), 193–208 (1999). <https://doi.org/10.1023/A:1006517625933>
12. Diebels, S.: Mikropolare Zweiphasenmodelle : Modellierung auf der Basis der Theorie Poröser Medien. Ph.D. thesis, Lehrstuhl für Kontinuumsmechanik, Universität Stuttgart (2000)
13. Diebels, S., Ehlers, W.: Dynamic analysis of a fully saturated porous medium accounting for geometrical and material non-linearities. *Int. J. Numer. Meth. Eng.* **39**(1), 81–97 (1996)
14. Dunwoody, N.T.: A thermomechanical theory of diffusion in solid-fluid mixtures. *Arch. Ration. Mech. Anal.* **38**(5), 348–371 (1970)
15. Ehlers, W., Markert, B., Diebels, S., Nodling, A.: Permeability studies on soft open-cell foams. *PAMM Proc. Appl. Math. Mech.* **2**, 162–163 (2003)
16. Engelhard, M., Lion, A.: Modelling the hydrothermomechanical properties of polymers close to glass transition. *ZAMM Z. Angew. Math. Mech.* **93**(2–3), 102–112 (2013)
17. Galeski, A., Argon, A.S., Cohen, R.E.: Changes in the morphology of bulk spherulitic nylon 6 due to plastic deformation. *Macromolecules* **21**(9), 2761–2770 (1988)
18. Goldschmidt, F., Diebels, S.: Modelling and numerical investigations of the mechanical behavior of polyurethane under the influence of moisture. *Arch. Appl. Mech.* **85**(8), 1035–1042 (2015). <https://doi.org/10.1007/s00419-014-0943-x>
19. Jöhrlitz, M., Diebels, S., Possart, W.: Investigation of the thermoviscoelastic material behaviour of adhesive bonds close to the glass transition temperature. *Arch. Appl. Mech.* **82**(8), 1089–1102 (2012). <https://doi.org/10.1007/s00419-012-0640-6>
20. Jöhrlitz, M., Lion, A.: Chemo-thermomechanical ageing of elastomers based on multiphase continuum mechanics. *Contin. Mech. Thermodyn.* **25**(5), 605–624 (2013)
21. Klepach, D., Zohdi, T.I.: Strain assisted diffusion: modeling and simulation of deformation-dependent diffusion in composite media. *Compos. B Eng.* **56**, 413–423 (2014). <https://doi.org/10.1016/j.compositesb.2013.08.035>
22. Kowalski, S.J.: Thermomechanics of the drying process of fluid-saturated porous media. *Dry. Technol.* **12**(3), 453–482 (1994). <https://doi.org/10.1080/07373939408959974>
23. Liu, I.S.: Method of lagrange multipliers for exploitation of the entropy principle. *Arch. Ration. Mech. Anal.* **46**, 131–148 (1972). <https://doi.org/10.1007/BF00250688>
24. Müller, I.: A thermodynamic theory of mixtures of fluids. *Arch. Ration. Mech. Anal.* **28**(1), 1–39 (1968). <https://doi.org/10.1007/BF00281561>
25. Nagamatsu, K.: On the viscoelastic properties of crystalline high polymers. *Kolloid Z.* **172**(2), 141 (1960)
26. Neff, F., Lion, A., Jöhrlitz, M.: Modelling diffusion induced swelling behaviour of natural rubber in an organic liquid. *ZAMM Z. Angew. Math. Mech.* **99**, 3 (2019)
27. Palabiyik, M., Bahadur, S.: Mechanical and tribological properties of polyamide 6 and high density polyethylene polyblends with and without compatibilizer. *Wear* **246**(1–2), 149–158 (2000)
28. Reese, S., Govindjee, S.: A theory of finite viscoelasticity and numerical aspects. *Int. J. Solids Struct.* **35**(26–27), 3455–3482 (1998). [https://doi.org/10.1016/s0020-7683\(97\)00217-5](https://doi.org/10.1016/s0020-7683(97)00217-5)
29. Sar, E.B., Fréour, S., Davies, P., Jacquemin, F.: Coupling moisture diffusion and internal mechanical states in polymers-A thermodynamical approach. *Eur. J. Mech. A Solids* **36**, 38–43 (2012)
30. Sharma, P., Sambale, A., Stommel, M., Maisl, M., Herrmann, H.G., Diebels, S.: Moisture transport in PA6 and its influence on the mechanical properties. *Continuum Mech. Therm.* **32**(2), 307–325 (2020). <https://doi.org/10.1007/s00161-019-00815-w>
31. Truesdell, C.: Rational Thermodynamics. Springer, New York (1984). <https://doi.org/10.1007/978-1-4612-5206-1>
32. Truesdell, C., Toupin, R.: The classical field theories. In: Principles of classical mechanics and field theory/Prinzipien der Klassischen Mechanik und Feldtheorie, vol. 2 / 3 / 1, pp. 226–858. Springer, Berlin, Heidelberg (1960)
33. Villani, A., Busso, E.P., Ammar, K., Forest, S., Geers, M.G.: A fully coupled diffusional-mechanical formulation: numerical implementation, analytical validation, and effects of plasticity on equilibrium. *Arch. Appl. Mech.* **84**(9–11), 1647–1664 (2014). <https://doi.org/10.1007/s00419-014-0860-z>